# Breakdown characteristics of carbon dioxide-ethane azeotropic mixtures near the critical point

Cite as: Phys. Fluids **32**, 053305 (2020); https://doi.org/10.1063/5.0004030 Submitted: 07 February 2020 . Accepted: 21 April 2020 . Published Online: 06 May 2020

📵 Jia Wei, Chanyeop Park, and 📵 Lukas Graber







ARTICLES YOU MAY BE INTERESTED IN

Modeling the dielectric strength variation of supercritical fluids driven by cluster formation near critical point

Physics of Fluids 32, 077101 (2020); https://doi.org/10.1063/5.0008848

Prediction of gas-liquid interface in oscillatory period
Physics of Fluids 32, 053304 (2020); https://doi.org/10.1063/1.5144708

Numerical investigation of bubble dynamics at a corner Physics of Fluids 32, 053306 (2020); https://doi.org/10.1063/1.5140740

Physics of Fluids
SPECIAL TOPIC: Tribute to
Frank M. White on his 88th Anniversary





## Breakdown characteristics of carbon dioxide-ethane azeotropic mixtures near the critical point

Cite as: Phys. Fluids 32, 053305 (2020); doi: 10.1063/5.0004030 Submitted: 7 February 2020 • Accepted: 21 April 2020 •







Published Online: 6 May 2020



Jia Wei, De Chanyeop Park, De and Lukas Graber



#### **AFFILIATIONS**

School of Electrical and Computer Engineering, Georgia Institute of Technology, Atlanta, Georgia 30313, USA

a) Author to whom correspondence should be addressed: jia.wei@gatech.edu

#### **ABSTRACT**

The properties of traditional dielectric media have been a major limiting factor impacting the design and operation of many applications spanning from particle accelerators over x-ray radiography and radiotherapy to electrical power systems. Supercritical fluids (SCFs) combine the properties of high dielectric strength, low viscosity, and excellent heat transfer capability. Here, we show, for the first time, the anomalous breakdown strength characteristics of SCF mixtures, such as carbon dioxide (CO<sub>2</sub>) and ethane (C<sub>2</sub>H<sub>6</sub>) mixtures and their azeotropic mixture under supercritical conditions. Our experiments suggest that the dielectric behavior deviates significantly from the established theory of gas discharge known by the work of Townsend and Paschen. Our results reveal that not only pure substances such as CO<sub>2</sub> exhibit a discontinuity of the dielectric strength near the critical point, but the supercritical mixture also manifests a discontinuity. The effect of random particle clustering in the pure substance and the mixture is observed, which impacts the mean free path of electrons. We present the measured breakdown voltage in a 0.1 mm gap with a uniform electric field over a wide range of mixture ratios and fluid densities and use a mathematical model by Stanley to show the density fluctuations that peak at around the critical point. By adjusting the mixing ratio, we prove that the mixture forms a useful combination of dielectric strengths and critical points and broadens the applicability of SC mixtures for a variety of

Published under license by AIP Publishing. https://doi.org/10.1063/5.0004030

Supercritical fluid (SCF), a state achieved when temperature and pressure are above the critical point of a substance, has drawn much attention because of its advantageous properties in chemical and material processing.<sup>1,2</sup> It has also been studied for use as an insulating and arc quenching medium due to its combined strengths of liquid and gaseous dielectrics. SCFs show exceptional dielectric strength, high heat transfer capability, and low viscosity. Many experimental and theoretical works on electric discharge under supercritical (SC) conditions have been researched in the literature. Specifically, Zhang et al. demonstrated that SC nitrogen (N2) shows excellent dielectric properties and recovery behavior from breakdown.<sup>3,4</sup> Kiyan et al. conducted research on the pre-breakdown and breakdown in SC carbon dioxide (CO2) with different electrode geometries. They also revealed the polarity effect in SC CO<sub>2</sub>.<sup>5-10</sup> Ito et al. performed measurements of breakdown voltages in SC CO2, SC water (H<sub>2</sub>O), and SC xenon (Xe) with 1 µm gap tungsten electrodes and discovered the decrease in the breakdown voltage near

the critical point. 11,12 In our previous study, a theoretical model was developed to describe the mechanism of electrical breakdown in SC CO<sub>2</sub> with molecular clusters formation.<sup>13</sup>

In all the investigations of the electric discharge plasmas generated in SC CO<sub>2</sub> and SC N<sub>2</sub> described above, there is no consideration of many other highly promising supercritical substances or mixtures even though the outstanding dielectric performance of supercritical fluids is demonstrated. Moreover, to the best of the authors' knowledge, there are no data on the dielectric performance of supercritical carbon dioxide-ethane (CO<sub>2</sub>-C<sub>2</sub>H<sub>6</sub>) mixtures, including their azeotropic mixture. Figure 1 summarizes the heat capacity, viscosity, and thermal conductivity of CO2 and C2H6 from 0 MPa to 20 MPa absolute pressures at a temperature of 308 K, and water at the same temperature is also added in this figure for comparison. 14 As shown in Fig. 1, properties such as viscosity, thermal conductivity, and heat capacity of SCFs are intermediate between those of liquids and gases. These properties are important for a dielectric medium,

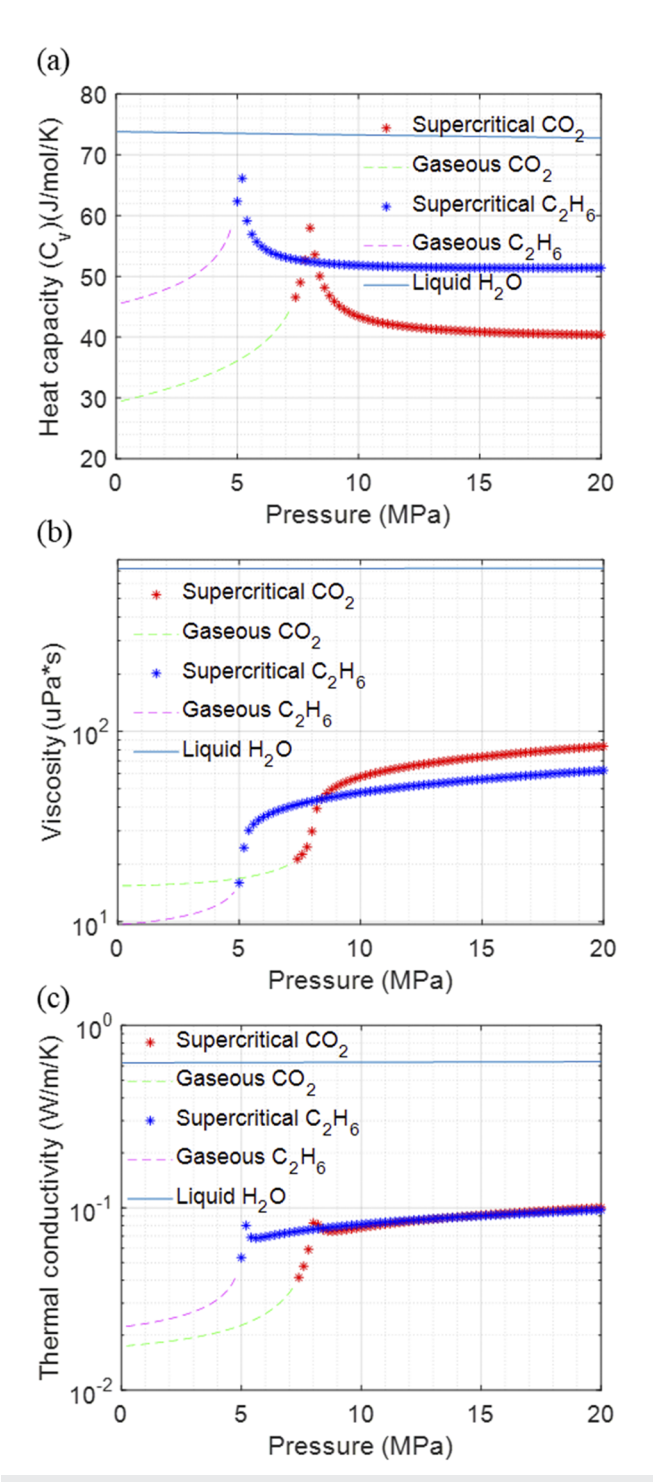


**FIG. 1**. Comparison of physical properties of carbon dioxide, ethane, and liquid water from 0 MPa to 20 MPa at 308 K: (a) heat capacity, (b) viscosity, and (c) thermal conductivity. Red stars represent carbon dioxide under the supercritical condition. Green dotted lines represent carbon dioxide in the gaseous phase. Blue stars represent ethane under the supercritical condition. Pink dotted lines represent ethane in the gaseous phase. Blue lines represent the thermodynamic properties of liquid water. Values are obtained from the NIST database. <sup>14</sup>

and hence, it is expected that such a medium can have many applications.

CO<sub>2</sub> has been one of the most frequently studied dielectric media due to its benign characteristics: high dielectric strength, nontoxic, low global warming potential (GWP), easily available, and low in cost. Furthermore, supercritical conditions are achievable with little effort ( $T_c = 304.1 \text{ K}$ ,  $P_c = 7.38 \text{ MPa}$ ). <sup>15</sup> C<sub>2</sub>H<sub>6</sub> was selected in this study for similar reasons. It is also non-toxic, has low GWP, and is easily available and low in cost. It also has a similar critical point to  $CO_2$  ( $T_c = 305.3$  K,  $P_c = 4.87$  MPa), which results in a critical point that is technically easier to achieve compared to pairs of substances with very different critical points. A more significant reason why C<sub>2</sub>H<sub>6</sub> was chosen in this study lies in the fact that C<sub>2</sub>H<sub>6</sub> forms an azeotropic mixture with CO<sub>2</sub>, which has a critical temperature that is lower than either of the constituents. 17 This property is important because it allows for a wider range of applications. Some reports in the literature suggest that such a mixture could provide improved properties and more potential applications than the pure substance. Kravanja et al. evaluated the heat transfer performance of the CO<sub>2</sub>-C<sub>2</sub>H<sub>6</sub> azeotropic mixture under SC conditions. Their results revealed that the heat transfer coefficient of the CO<sub>2</sub>-C<sub>2</sub>H<sub>6</sub> azeotropic mixture fell between the values for pure CO<sub>2</sub> and C<sub>2</sub>H<sub>6</sub>, which proves that such a mixture has the capability to be used as an alternative fluid in heat power cycles. 18 Considering its thermal properties, the investigation of the dielectric properties of such mixtures would be an imperative task in order to show the feasibility of a SCF as a promising dielectric medium.

Figure 2 shows the density vs pressure diagram of both  $\rm CO_2$  and  $\rm C_2H_6$  by two isothermal lines. Experiments were conducted at a constant temperature of 308 K, and the breakdown voltages were measured from gaseous to SC conditions. Besides the pure substances, it is also necessary to know the critical points of the mixtures with different mixing ratios so that the thermodynamic

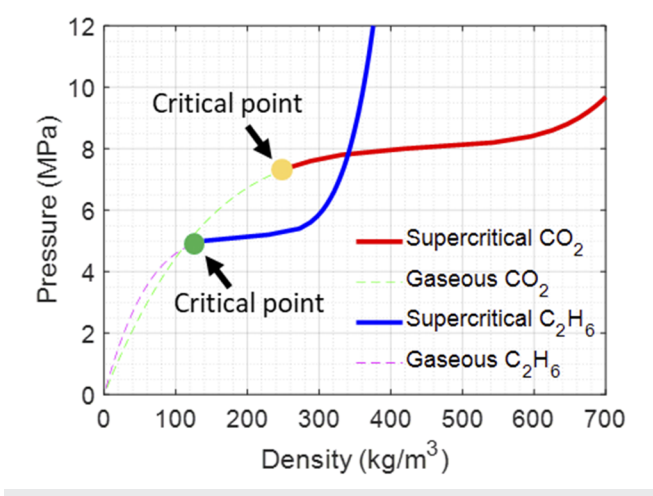


**FIG. 2.** Phase diagram of carbon dioxide and ethane. Experimental conditions represented by isothermal lines of  $CO_2$  and  $C_2H_6$  density–pressure diagram at 308 K ( $T_r = T/T_c = 1.012$ ). The red line represents carbon dioxide under the supercritical condition. The dotted green line represents carbon dioxide in the gaseous phase. The solid blue line represents ethane under the supercritical condition. The pink dotted line represents ethane in the gaseous phase.

phase inside the high pressure chamber can be confirmed. A high pressure optical vessel was used to observe the phase transition of the mixtures visually. The critical points of the mixtures from the optical diagnostics were in good agreement with the critical points calculated from the PSRK (predictive Soave–Redlich–Kwong) model. The comparison of the critical points of the mixtures with respect to the mass fraction will be discussed in the following paragraphs.

The breakdown voltage measurements of pure CO<sub>2</sub> were carried out at a temperature of 308 K from the gaseous phase to SC condition, as shown in Fig. 2. Figure 3(a) shows the measured breakdown voltages as a function of the pressure, and Fig. 3(b) shows the measured breakdown voltages as a function of the density. The average breakdown voltage of 15 measurements and their scattering data under one experimental condition are represented by an open circle and a vertical error bar, respectively. The density values were calculated by using the equation of state (EoS)<sup>20</sup> from pressure and temperature during the experiment and confirmed by weighing the mass of the substance inside the high pressure chamber.

Clearly, the measured breakdown voltage increases with the density of  $CO_2$  and scatters more in the supercritical region. An obvious discontinuity of the slope can be observed near the critical point where the substance experiences a phase change. Under the SC condition, the composition of the fluid is characterized by inhomogeneity in the molecular distribution due to the distinct clusters of molecules. Especially, under the conditions close to the critical point, the density fluctuation  $F_D$  increases substantially due to repeated aggregation and dispersion of clusters, which influences the breakdown strength significantly. The density fluctuation  $F_D$  is defined by defined by  $F_D$ 

$$F_D = \frac{\left\langle (N - \langle N \rangle)^2 \right\rangle}{\langle N \rangle} = \frac{(n_s V)^2}{n_{ave} V} = \frac{k_T}{k_T^0},\tag{1}$$

where N is the total number of particles in a given volume V,  $\langle N \rangle$  is the average of N,  $n_s$  is the standard deviation of the local number density,  $n_{ave}$  is the average number density,  $k_T$  is the isothermal compressibility, and  $k_T^0$  is the value of  $k_T$  for an ideal gas. A larger  $F_D$  means larger density fluctuations, and  $F_D$  reaches local maxima at the critical point.

The density inhomogeneity is caused by the clustering effect, which forms a large mean free path where electrons could gain enough energy and ionize particles. Although the phenomenon of the discontinuity in breakdown vs density near the critical point in the experiment is pronounced, the decrease in the breakdown voltage near the critical point reported by Ito et al. was not observed, which was expected because the gap length in this study is relatively large. This is because when the gap distance decreases, the volume of the locally low-density domain at the breakdown V also decreases. This causes  $n_s/n_{ave}$  to increase, as shown in Eq. (1). This indicates that the effect of the density fluctuations on the breakdown voltage becomes more significant with a decrease in the gap distance.<sup>22</sup> Moreover, in the case when discharges happen under the condition of being close to the critical point, clustering and density fluctuation  $F_D$  decrease due to the increase in the local temperature caused by discharges. If the gap length is smaller than 1  $\mu$ m, the cluster structure can be preserved because more effective heat dissipation

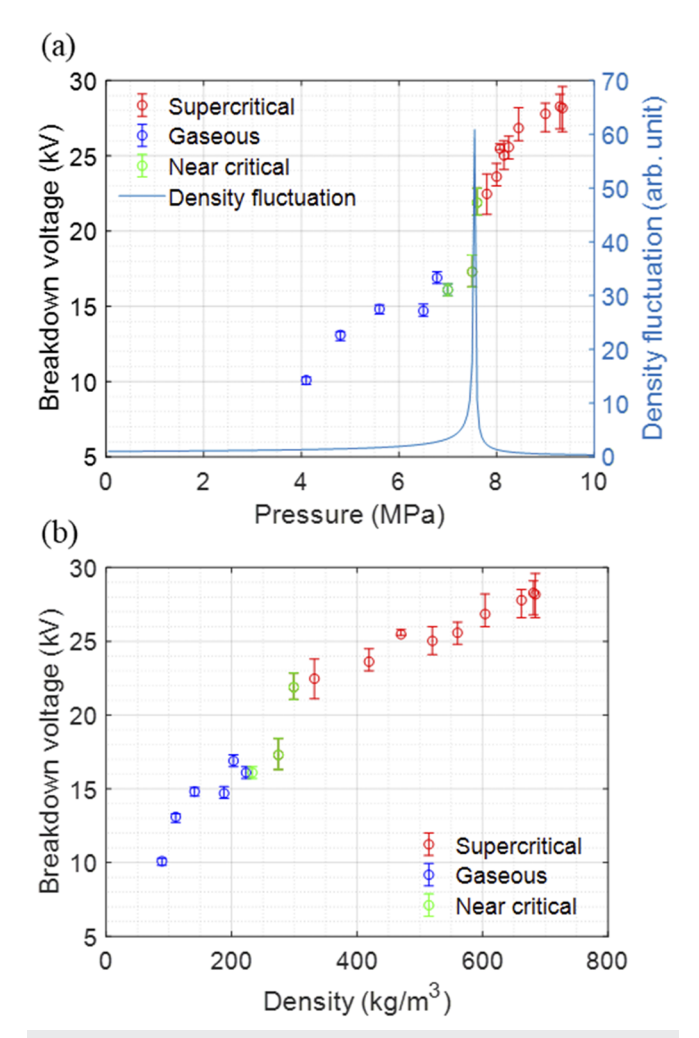


FIG. 3. Experimental results for the dielectric strength of supercritical carbon dioxide up to 10 MPa. (a) Breakdown voltage as a function of the pressure of  $CO_2$  in a uniform electric field at a 0.1 mm gap. The right y-axis indicates the density fluctuation  $F_D$ , which quantifies the molecular clustering.  $F_D$  values are calculated by Eq. (1), and the isothermal compressibility  $k_T = k_S C_p/C_V$ , where  $k_S$  is the isentropic compressibility,  $C_p$  is the heat capacity for the isobaric process, and  $C_V$  is the heat capacity for the isochoric process. (b) Experimental values of the breakdown voltages as a function of the density of  $CO_2$ . Red circles represent the average breakdown voltage in the supercritical condition. Blue circles represent the average breakdown voltage in the gaseous phase. Green circles represent the average breakdown voltage measured near the critical point of carbon dioxide. Vertical error bars represent the corresponding experimental scattering data.

is enabled by the large specific surface area.<sup>24</sup> Thus, a reduction in the breakdown voltage can be observed.

The reason for the deviation between the breakdown voltage in SCFs and the gaseous state is that the gaseous discharge theory cannot explain the situation when the mean free path of electrons in SCFs starts to decrease. In this circumstance, SCFs deviate considerably from the ideal gas behavior, and a small change in the pressure causes a large change in the density. Paschen's law

cannot precisely predict the breakdown voltage in high pressure gases and SCFs. Specifically, Paschen's law fails to estimate the breakdown characteristics in the compressed medium when the electric field is of the order 10–20 kV/mm. The deviation from Paschen's law depends on the material, separation and area of the electrodes, and particles of dusts near the electrodes. Similarly, the failure of the Townsend mechanism for SCFs is that the Townsend theory does not take the field emission of electrons from the cathode in a high density situation into consideration. <sup>25</sup>

To identify the state of the mixture inside the high pressure chamber, the critical points of the mixtures with different mixing ratios need to be determined. Horstmann et al. conducted the experimental determination of the critical line for CO2-C2H6 mixtures and compared their results with the PSRK model. 19 The PSRK model is able to reliably predict the thermodynamic properties of carbon dioxide and alkanes by using one pair of temperature-dependent group interaction parameters. Such a model has been widely used in process simulators because it combines the advantages of the EoS, the local composition concept, and the group contribution approach. Optical diagnostics were conducted by using an optical chamber to replicate the experimental conditions considering mixing ratios and densities so that the critical points of the mixtures can be measured. Table I compares the critical points observed from the optical cell and calculated from the PSRK model with respect to the mass fraction. The error between two methods, as shown in Table I, is expected to be caused in part due to the presence of impurities.

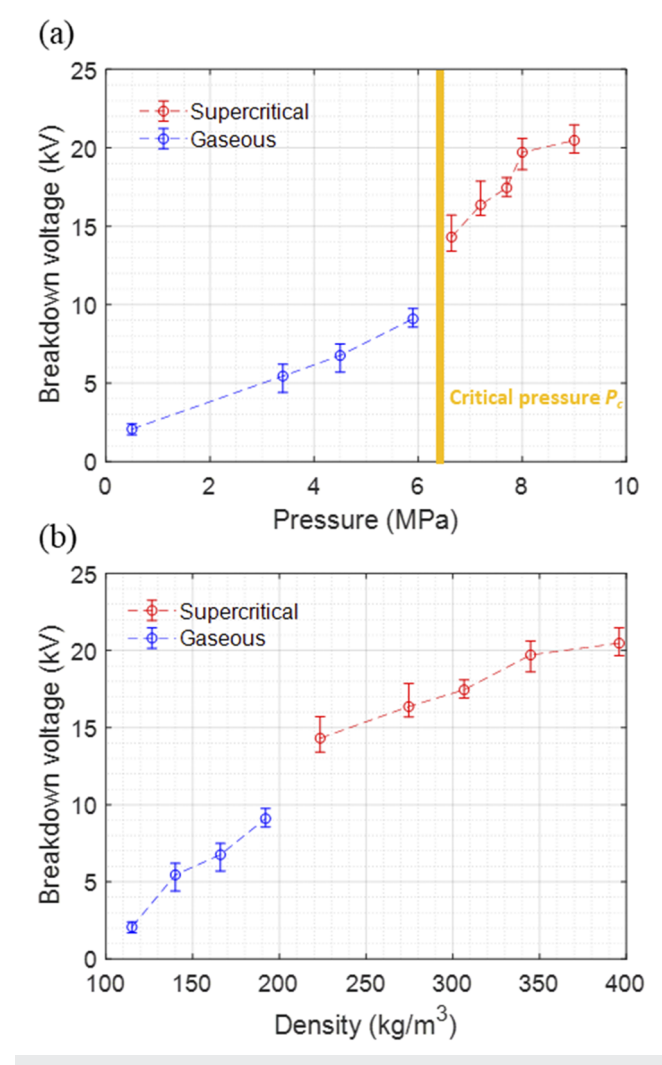
To ensure consistency in the experimental results with the pure CO<sub>2</sub> data, the gap between the copper electrodes was also set to 0.1 mm. C<sub>2</sub>H<sub>6</sub> mass percentages of 10%, 25% (azeotropic), <sup>18</sup> 30%, 40%, and 50% were tested in the breakdown experiment. An oily substance between two electrodes was observed after the first breakdown when the  $C_2H_6$  mass percentage ( $\omega$ ) reaches beyond 60%. Rosocha et al. conducted experiments to determine the decomposition of C<sub>2</sub>H<sub>6</sub> under dielectric-barrier discharges at 77.3 kPa and a temperature range of 293-323 K. The primary decomposition products they found were molecular hydrogen (H<sub>2</sub>), methane (CH<sub>4</sub>), acetylene ( $C_2H_2$ ), and ethylene ( $C_2H_4$ ). Oro et al. also observed a similar phenomenon that organic compounds are formed under the influence of electric discharges with C<sub>2</sub>H<sub>6</sub> at a pressure range of 10-30 kPa at 303 K. Their results indicate that the product caused by the electric discharge could be a highly cross-linked polyethylene-type polymer.<sup>2</sup>

**TABLE I.** Comparison of the critical temperature  $T_c$  and critical pressure  $P_c$  for  $\omega C_2 H_6 + (1 - \omega)CO_2$ .

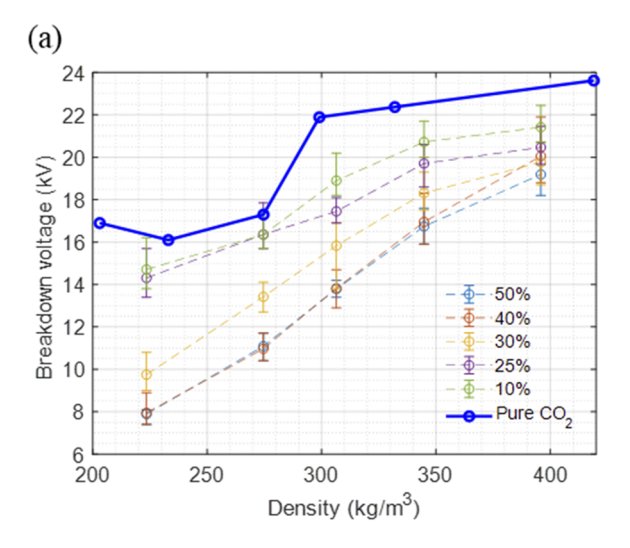
ω	Optical diagnostics		PSRK model	
	$T_c$ (K)	$P_c$ (MPa)	$T_c$ (K)	$P_c$ (MPa)
0.1	300.0	6.75	297.5	6.73
0.25	294.5	6.50	292.0	6.35
0.3	294.0	6.05	291.2	5.94
0.4	293.5	5.82	291.5	5.70
0.5	293.0	5.55	292.0	5.52

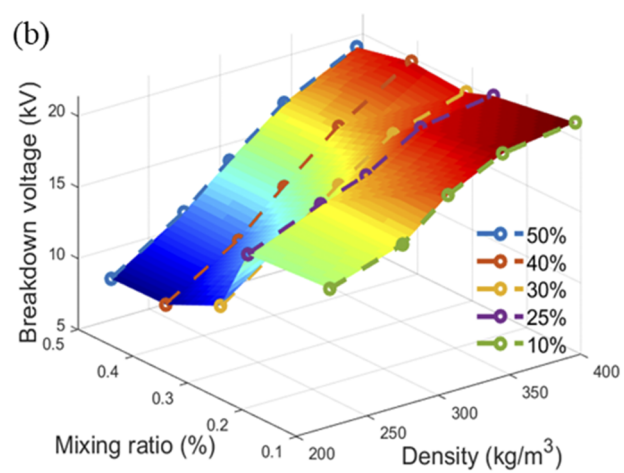
A similar anomalous breakdown behavior near the critical point of pure  $CO_2$ , as shown in Fig. 3, was also observed in the  $CO_2$ – $C_2H_6$  mixture at the azeotropic mixing ratio, as shown in Fig. 4. It should be noted that the discontinuity of breakdown voltages happens at the locus of the states where the scale and the magnitude of the density fluctuation reach maxima on the isothermal line. It also represents a boundary that divides the supercritical region into liquid-like and gas-like phases. <sup>28,29</sup> According to the experimental condition in this study, since experiments were conducted under the isothermal condition of 308 K, the density fluctuation  $F_D$  is expected to peak slightly above 6.5 MPa, which is the observed critical pressure.

Figure 5(a) shows a 2D plot of the measured breakdown voltage at different mixing ratios as a function of the density. A solid



**FIG. 4**. (a) Breakdown voltage as a function of the pressure of the  $CO_2-C_2H_6$  mixture at the azeotropic mixing ratio (25% mass fraction of  $C_2H_6$ ) in a uniform electric field, at a temperature of 308 K in (a) 0.1 mm gap. (b) Breakdown voltage as a function of the density of the  $CO_2-C_2H_6$  mixture at the azeotropic mixing ratio.





**FIG. 5**. (a) A 2D plot of the breakdown voltage at different mixing ratios as a function of the density. The solid blue line indicates the average of the measurement data of pure  $CO_2$ . (b) Breakdown voltage at different mixing ratios as a function of the density at a temperature of 308 K.  $\omega$ : the mass percentage of  $C_2H_6$ . The  $C_2H_6$  mixing ratio varies from 10% to 50% by mass into  $CO_2$ .

blue line indicates the average of the measurement data of pure  $CO_2$ . Figure 5(b) presented a 3D plot of all the measured breakdown voltages of supercritical  $CO_2$ – $C_2H_6$  mixtures at different mixing ratios as a function of the density. All the breakdown values presented in Fig. 5(b) were measured under the supercritical condition. For all the mixtures at different mixing ratios, the highest dielectric strength is shown at the highest density of 396 kg/m³ and the lowest at 223 kg/m³. In addition, for all five SCF mixtures, the breakdown voltage decreases with an increase in the  $C_2H_6$  mass fraction. The transition between 25% and 30% of the  $C_2H_6$  mass fraction in Fig. 5 shows a steep decrease, especially in the lower density region. Such a transition can be attributed to the fact that under different  $C_2H_6$  mass fractions, the locations where density fluctuations reach maxima can also be shifted. In this situation, the large inhomogeneity in the molecular distribution caused by the rapid and repeated

aggregation and dispersion of clusters can be shown from the unstable breakdown voltages. Specifically, we speculate that our experimental result indicates that the samples of C<sub>2</sub>H<sub>6</sub> concentration at 25% and 30% are closer to the supercritical liquid-gas boundary line. Also, the measured breakdown voltage of the mixtures scatters more widely compared to the values of pure CO<sub>2</sub>. In the lower density region between 220 kg/m<sup>3</sup> and 300 kg/m<sup>3</sup>, the difference in the breakdown voltages of the mixtures tends to be more obvious than those in the higher density region. The data also indicate that the breakdown voltages of different mixing ratios saturate at higher densities. The breakdown voltage of the mixtures in the lower density region also shows a more pronounced reduction compared to pure CO<sub>2</sub>. For the azeotropic mixture of CO<sub>2</sub> and C<sub>2</sub>H<sub>6</sub> (25% mass fraction of C<sub>2</sub>H<sub>6</sub> and 75% mass fraction of CO<sub>2</sub>), the breakdown voltage shows an average of 20.5% reduction compared to the dielectric strength of pure  $CO_2$  in the vicinity of the critical point of  $CO_2$ . In the higher density region far away from the critical point, the reduction in dielectric strength of the mixture drops to about 13.5%compared to pure CO<sub>2</sub>.

Our study found that the anomalous breakdown characteristics discovered in the pure SCF are also observable in binary mixtures of supercritical fluids at various azeotropic mixture ratios. The similar behavior suggests that the unstable molecular clustering could significantly affect the discharge phenomenon observed in both pure SCFs and supercritical mixtures. Unique properties of SCF mixtures with respect to the dielectric strength, viscosity, specific heat capacity, and tunable critical point are expected to attract interest for a wide range of applications. Besides the applications in power and energy, where they could be used for switchgear and electrostatic machines, 30–32 SCF mixtures could also enable affordable van-de-Graaff generators for particle accelerators used in high energy physics and medical applications, such as radiation therapy. 33,34

### **REFERENCES**

- <sup>1</sup> A. A. Clifford and J. R. Williams, Supercritical Fluid Methods and Protocols (Springer, 2000), p. 1.
- <sup>2</sup>M. McHugh and V. Krukonis, Supercritical Fluid Extraction: Principles and Practice (Elsevier, 2013).
- <sup>3</sup> J. Zhang, E. J. M. van Heesch, F. J. C. M. Beckers, A. J. M. Pemen, R. P. P. Smeets, T. Namihira, and A. H. Markosyan, "Breakdown strength and dielectric recovery in a high pressure supercritical nitrogen switch," IEEE Trans. Dielextr. Electr. Insul. 22, 1823 (2015).
- <sup>4</sup>J. Zhang, B. van Heesch, F. Beckers, T. Huiskamp, and G. Pemen, "Breakdown voltage and recovery rate estimation of a supercritical nitrogen plasma switch," IEEE Trans. Plasma Sci. **42**, 376 (2014).
- <sup>5</sup>T. Kiyan, A. Uemura, B. C. Roy, T. Namihira, M. Hara, M. Sasaki, M. Goto, and H. Akiyama, "Negative DC prebreakdown phenomena and breakdown-voltage characteristics of pressurized carbon dioxide up to supercritical conditions," IEEE Trans. Plasma Sci. 35, 656 (2007).
- <sup>6</sup>T. Kiyan, M. Takade, T. Namihira, M. Hara, M. Sasaki, M. Goto, and H. Akiyama, "Polarity effect in DC breakdown voltage characteristics of pressurized carbon dioxide up to supercritical conditions," IEEE Trans. Plasma Sci. 36, 821 (2008).
- <sup>7</sup>T. Kiyan, T. Ihara, S. Kameda, T. Furusato, M. Hara, and H. Akiyama, "Weibull statistical analysis of pulsed breakdown voltages in high-pressure carbon dioxide including supercritical phase," IEEE Trans. Plasma Sci. 39, 1729 (2011).
- <sup>8</sup>T. Furusato, N. Ashizuka, T. Kamagahara, Y. Matsuda, T. Yamashita, M. Sasaki, T. Kiyan, and Y. Inada, "Anomalous plasma temperature at supercritical phase of pressurized CO," IEEE Trans. Dielextr. Electr. Insul. 25, 1807 (2018).

- <sup>9</sup>T. Furusato, N. Ashizuka, T. Kamagahara, T. Fujishima, T. Yamashita, M. Sasaki, and T. Kiyan, *Spectroscopic Characteristics of Pulsed Arc Discharge in High-Pressure CO<sub>2</sub> up to Supercritical Phase* (IEEE, 2017), p. 1.
- <sup>10</sup>T. Kamagahara, N. Ashizuka, T. Furusato, T. Fujishima, T. Yamashita, M. Sasaki, and T. Kiyan, *Investigation of Pulsed Breakdown Characteristics in High-Pressure CO<sub>2</sub> Including Supercritical Phase under Non-Uniform Electric Field* (IEEE, 2017), p. 1.
- <sup>11</sup>T. Ito and K. Terashima, "Generation of micrometer-scale discharge in a supercritical fluid environment," Appl. Phys. Lett. 80, 2854 (2002).
- <sup>12</sup>T. Ito, H. Fujiwara, and K. Terashima, "Decrease of breakdown voltages for micrometer-scale gap electrodes for carbon dioxide near the critical point: Temperature and pressure dependences," J. Appl. Phys. 94, 5411 (2003).
- <sup>13</sup>Y. Tian, J. Wei, C. Park, Z. Wang, and L. Graber, *Modelling of Electrical Breakdown in Supercritical CO*<sub>2</sub> with Molecular Clusters Formation (IEEE, 2018), p. 992.
- p. 992.

  14 E. Lemmon, M. McLinden, D. Friend, P. Linstrom, and W. Mallard, NIST Chemistry WebBook, NIST Standard Reference Database Number 69 (National Institute of Standards and Technology, Gaithersburg, 2011).
- <sup>15</sup>Y. Suehiro, M. Nakajima, K. Yamada, and M. Uematsu, "Critical parameters of  $\{xCO_2 + (1-x)CHF_3\}$  for x = (1.0000, 0.7496, 0.5013, and 0.2522)," J. Chem. Thermodyn. **28**, 1153 (1996).
- <sup>16</sup>D. Ambrose and C. Tsonopoulos, "Vapor-liquid critical properties of elements and compounds. 2. Normal alkanes," J. Chem. Eng. Data 40, 531 (1995).
- <sup>17</sup>J. Kuenen, "XXVII. Experiments on the condensation and critical phenomena of some substances and mixtures," London, Edinburgh, Dublin Philos. Mag. J. Sci. 44, 174 (1897).
- $^{18}$ G. Kravanja, G. Zajc, Ž. Knez, M. Škerget, S. Marčič, and M. H. Knez, "Heat transfer performance of  $CO_2$ , ethane and their azeotropic mixture under supercritical conditions," Energy **152**, 190 (2018).
- <sup>19</sup>S. Horstmann, K. Fischer, J. Gmehling, and P. Kolář, "Experimental determination of the critical line for (carbon dioxide + ethane) and calculation of various thermodynamic properties for (carbon dioxide + *n*-alkane) using the PSRK model," J. Chem. Thermodyn. **32**, 451 (2000).
- <sup>20</sup>R. Span and W. Wagner, "A new equation of state for carbon dioxide covering the fluid region from the triple-point temperature to 1100 K at pressures up to 800 MPa," J. Phys. Chem. Ref. Data 25, 1509 (1996).
- <sup>21</sup> K. Karalis, C. Ludwig, and B. Niceno, "Supercritical water anomalies in the vicinity of the Widom line," Sci. Rep. 9, 15731 (2019).

- <sup>22</sup>H. E. Stanley, *Phase Transitions and Critical Phenomena* (Clarendon Press, Oxford, 1971).
- <sup>23</sup>H. Muneoka, K. Urabe, S. Stauss, and K. Terashima, "Micrometer-scale electrical breakdown in high-density fluids with large density fluctuations: Numerical model and experimental assessment," Phys. Rev. E 91, 042316 (2015).
- <sup>24</sup>S. Stauss, H. Muneoka, K. Urabe, and K. Terashima, "Review of electric discharge microplasmas generated in highly fluctuating fluids: Characteristics and application to nanomaterials synthesis," Phys. Plasmas 22, 057103 (2015).
- <sup>25</sup>A. H. Cookson, Electrical Breakdown for Uniform Fields in Compressed Gases (IET, 1970), p. 269.
- <sup>26</sup>L. A. Rosocha, Y. Kim, G. K. Anderson, J. O. Lee, and S. Abbate, "Decomposition of ethane in atmospheric-pressure dielectric-barrier discharges: Experiments," IEEE Trans. Plasma Sci. 34, 2526 (2006).
- <sup>27</sup> J. Oro, "Synthesis of organic compounds by high-energy electrons," Nature 197, 971 (1963).
- <sup>28</sup>T. Sato, M. Sugiyama, K. Itoh, K. Mori, T. Fukunaga, M. Misawa, T. Otomo, and S. Takata, "Structural difference between liquidlike and gaslike phases in supercritical fluid," Phys. Rev. E 78, 051503 (2008).
- <sup>29</sup>S. Artemenko, P. Krijgsman, and V. Mazur, "The Widom line for supercritical fluids," J. Mol. Liq. **238**, 122 (2017).
- <sup>30</sup>C. Xu, T. Damle, and L. Graber, A Survey on Mechanical Switches for Hybrid Circuit Breakers (IEEE, 2019), p. 1.
- <sup>31</sup>B. Ge and D. C. Ludois, "Dielectric liquids for enhanced field force in macro scale direct drive electrostatic actuators and rotating machinery," IEEE Trans. Dielextr. Electr. Insul. 23, 1924 (2016).
- <sup>32</sup>B. Ge and D. C. Ludois, "Design concepts for a fluid-filled three-phase axial-peg-style electrostatic rotating machine utilizing variable elastance," IEEE Trans. Ind. Appl. **52**, 2156 (2016).
- <sup>33</sup>J. Constanzo, M. Fallavier, G. Alphonse, C. Bernard, P. Battiston-Montagne, C. Rodriguez-Lafrasse, D. Dauvergne, and M. Beuve, "Radiograaff, a proton irradiation facility for radiobiological studies at a 4 MV Van de Graaff accelerator," Nucl. Instrum. Methods Phys. Res., Sect. B 334, 52 (2014).
- <sup>34</sup>M. Belli, R. Cherubini, G. Galeazzi, S. Mazzucato, G. Moschini, O. Sapora, G. Simone, and M. Tabocchini, "Proton irradiation facility for radiobiological studies at a 7 MV Van de Graaff accelerator," Nucl. Instrum. Methods Phys. Res., Sect. A 256, 576 (1987).